European Journal of Pharmaceutics and Biopharmaceutics 108 (2016) 226–234

Contents lists available at ScienceDirect

European Journal of Pharmaceutics and Biopharmaceutics

journal homepage: www.elsevier.com/locate/ejpb

Research paper

# A novel oral iron-complex formulation: Encapsulation of hemin in polymeric micelles and its *in vitro* absorption

Kimberley Span [1], Johan J.F. Verhoef [1], Hedi Hunt, Cornelus F. van Nostrum, Vera Brinks, Huub Schellekens, Wim E. Hennink *

*Department of Pharmaceutics, Utrecht Institute for Pharmaceutical Sciences (UIPS), Utrecht University, Utrecht, The Netherlands*

ARTICLE INFO

*Article history:*
Received 8 April 2016
Revised 1 September 2016
Accepted in revised form 2 September 2016
Available online 4 September 2016

*Keywords:*
Polymeric micelle
Nanomedicine
Caco2
Solubilization
Heme
Anemia

ABSTRACT

Anemia resulting from iron deficiency is one of the most prevalent diseases in the world. As iron has important roles in several biological processes such as oxygen transport, DNA synthesis and cell growth, there is a high need for iron therapies that result in high iron bioavailability with minimal toxic effects to treat patients suffering from anemia. This study aims to develop a novel oral iron-complex formulation based on hemin-loaded polymeric micelles composed of the biodegradable and thermosensitive polymer methoxy-poly(ethylene glycol)-b-poly[*N*-(2-hydroxypropyl)methacrylamide-dilactate], abbreviated as mPEG-*b*-p(HPMAm-Lac$_2$). Hemin-loaded micelles were prepared by addition of hemin dissolved in DMSO:DMF (1:9, one volume) to an aqueous polymer solution (nine volumes) of mPEG-*b*-p(HPMAm-Lac$_2$) followed by rapidly heating the mixture at 50 °C to form hemin-loaded micelles that remain intact at room and physiological temperature. The highest loading capacity for hemin in mPEG-*b*-p(HPMAm-Lac$_2$) micelles was 3.9%. The average particle diameter of the hemin-micelles ranged from 75 to 140 nm, depending on the concentration of hemin solution that was used to prepare the micelles. The hemin-loaded micelles were stable at pH 2 for at least 3 h which covers the residence time of the formulation in the stomach after oral administration and up to 17 h at pH 7.4 which is sufficient time for uptake of the micelles by the enterocytes. Importantly, incubation of Caco-2 cells with hemin-micelles for 24 h at 37 °C resulted in ferritin levels of 2500 ng/mg protein which is about 10-fold higher than levels observed in cells incubated with iron sulfate under the same conditions. The hemin formulation also demonstrated superior cell viability compared to iron sulfate with and without ascorbic acid. The study presented here demonstrates the development of a promising novel iron complex for oral delivery.

© 2016 Elsevier B.V. All rights reserved.

## 1. Introduction

Anemia is one of the most common health problems at present. According to the World Health Organization the prevalence of anemia is dependent on ethnic groups and geographic location, but it is assumed that 50% of these cases are because of iron deficiency [1]. This occurrence is similar for both developing and developed nations and can arise due to various reasons such as pregnancy, growth in children and diseases that cause low iron bioavailability from the diet [2–4].

A healthy iron metabolism is important as iron is the main mineral involved in oxygen transport, DNA synthesis, cell growth and survival [5,6]. The iron homeostasis is primarily regulated by intestinal absorption as the uptake of iron takes place predominately in the duodenum and upper jejunum by enterocytes. This absorption is regulated by the hormone hepcidin that is produced in hepatocytes of the liver and binds to the iron transporter protein ferroportin that carries iron from the duodenal enterocytes into the circulation [7]. It is known that hepcidin binding to the iron transporter leads to its degradation; therefore, augmented hepcidin production results in less ferroportin and thus less iron transportation (export). As a consequence a decrease in iron absorption and efflux from the enterocytes occurs. This incidence results in a disturbed iron homeostasis and ultimately could cause less iron in the circulation [8–10]. Due to the importance of a balanced iron metabolism, it is of interest to develop therapies that can remediate iron deficiency. There are two forms of dietary iron, namely non-heme iron that is present in vegetables and grains, and there is heme iron that is predominately found in red meat in the form of hemoglobin and myoglobin [11]. It is known that even though the prevalence of non-heme iron is higher than the heme form, the latter is being absorbed up to 30% more effectively [12].

* Corresponding author.
*E-mail address:* W.E.Hennink@uu.nl (W.E. Hennink).
[1] Equal contribution.

http://dx.doi.org/10.1016/j.ejpb.2016.09.002
0939-6411/© 2016 Elsevier B.V. All rights reserved.

Nevertheless, because non-heme iron supplements are relatively cheap and easy to produce, the pharmaceutical industry has developed several oral formulations based on iron salts such as iron sulfate. However, these formulations are associated with various side effects such as gastrointestinal disturbances which are probably caused by the redundant amount of iron in the preparations that remain unabsorbed in the colon [13]. There is consequently an urgent need for more advanced oral preparations with higher bioavailability and less side effects. Many studies have explored the possibilities of novel therapies based on non-heme iron, but even though there are some heme-iron based oral iron medications on the market such as Proferrin (heme iron polypeptide), far less research has been done exploiting heme-iron for oral supplementation [6,14]. Unlike non-heme iron that is taken up by enterocytes via the divalent metal transporter 1 (DMT1), the exact uptake mechanism for heme remains elusive. It is, however, generally accepted that heme binds to the brush border membrane of the duodenum enterocytes and is subsequently transported by a different transporter as non-heme iron through the cell membrane to the cytoplasm [15–17]. The assumption that heme is recognized by a heme-transporter opens possibilities to investigate other sources for iron supplementation containing structures similar to heme such as ferric protoporphyrin IX chloride (hemin). Hemin in contrast to heme contains a chloro ligand attached to the iron center (structure is shown in Fig. 1). This compound is essentially insoluble in water of neutral pH and soluble in solutions of sodium hydroxide due to the substitution of the chloro ligand by a hydroxyl group resulting in the formation of hematin [18]. The prominent factors for the development of a novel oral therapy would be improving the stability, bioavailability and solubility of the iron supplement [19]. Thus, in order to exploit hemin for oral iron therapy, the first challenge to tackle is to solubilize it in aqueous medium of physiological pH. Moreover a suitable formulation has to resist the harsh environment of the gastrointestinal tract.

In particular nano-sized drug delivery systems have shown to be able to encapsulate several hydrophobic substances while increasing the uptake of the loaded drug and protecting it from degradation while passing through the gastrointestinal tract [20–22]. There is a wide range of nanoparticles based on liposomes and on natural as well as synthetic polymers that have been investigated for the encapsulation of hydrophobic drugs [23–25]. Within our department a novel class of thermosensitive biodegradable block copolymers based on methoxy-poly(ethylene glycol)-b-poly [*N*-(2-hydroxypropyl)methacrylamide-dilactate] (mPEG-*b*-p (HPMAm-$Lac_2$) has been developed, which under certain conditions form micelles consisting of a hydrophobic core, in which hydrophobic drugs can be solubilized and a hydrophilic corona, making these particles water dispersible [26,27,30,31]. mPEG-b-(HPMAm-Lac2) consists of the hydrophilic polymer mPEG and poly(HPMAm-Lac2). The latter polymer is thermosensitive and, when dissolved in water, exhibits a lower critical solution temperature (LCST) [27], as has also been described for polymers such as poly(*N*-isopropylacrylamide) and elastin-like peptides [28,29]. Below the LCST poly(HPMAm-Lac2) 13 °C, water molecules are bound to the polymer chains and prevent intra- and inter polymer interactions resulting in a water-soluble polymer. When the polymer solution is heated above its LCST, water is expelled and the polymer chains become hydrophobic resulting in precipitation [27]. Therefore, in the present study we investigated whether these micelles can also encapsulate the hydrophobic hemin and thus be used as a potential oral iron formulation. To this end, hemin was encapsulated in mPEG-*b*-p(HPMAm-$Lac_2$) micelles via a rapid heating method. The formed micelles were characterized for encapsulation efficiency, loading capacity and particle size. Furthermore, the stability of the loaded micelles at different pH and also the physical state of hemin within the micelles were investigated. Finally, Caco-2 cells were incubated with the micelles to assess iron uptake in comparison with the commonly used iron supplement, iron sulfate.

## 2. Materials and methods

### 2.1. Materials

Hemin (molecular weight = 651.9 g/mol), ammonium acetate, iron (II) sulfate heptahydrate; $FeSO_4 \cdot 7H_2O$, sodium hydroxide, sodium bicarbonate, ascorbic acid, saponin and tetrazolium salt XTT (sodium 2,3-bis(2-methoxy-4-nitro-5-sulfophenyl)-2H-tetrazolium-5-carboxanilide) were all purchased from Sigma Aldrich (Zwijndrecht, The Netherlands). Dimethylsulfoxide (DMSO) and dimethylformamide (DMF) were obtained from Biosolve Ltd. (Valkenswaard, The Netherlands). Phosphate buffered saline (PBS) pH 7.4 containing per liter 8.2 g NaCl, 3.1 g $Na_2HPO_4 \cdot 12H_2O$ and 0.3 g $NaH_2PO_4 \cdot 2H_2O$ was from Braun Melsungen AG (Melsungen, Germany).

Methoxy-poly(ethylene glycol)-*b*-poly[*N*-(2-hydroxypropyl)methacrylamide-dilactate] (abbreviated as mPEG-*b*-p(HPMAm-Lac2); Molecular weight of mPEG = 5000 g/mol) was synthesized as described by Soga et al. [26]. Regenerated cellulose syringe filters (0.45 μm) were purchased from Grace Davison Discovery Science. Vivaspin centrifugal concentrator tubes with 50,000 MWCO filter were obtained from Sartorius AG (Goettingen, Germany). The Caco-2 cell line was generously provided by M.A.M Oosterveer-van der Doelen (Faculty of Veterinary Medicine, Utrecht University). Dulbecco's Modified Eagle's Medium, Minimum Essential Medium, antibiotic antimycotic cell culture solution consisting of amphotericin B and penicillin, non-essential amino acids and RIPA buffer were obtained from Invitrogen (Breda, The Netherlands). Micro BCA™ protein assay and Ferritin Human ELISA kit (ab 108837) were purchased from Pierce (Rockford, USA) and Abcam (Cambridge, United Kingdom). Rabbit polyclonal anti-LAMP1 IgG-Lysosome Marker (ab24170) and Goat polyclonal anti-Rabbit IgG H&L (Alexa Fluor® 488) (ab150077) were purchased from Abcam (Cambridge, United Kingdom). Methacryloxyethyl thiocarbamoyl rhodamine B was purchased from Polysciences Europe. Leica Confocal microscopy with Leica application suite advanced fluorescence (LAS AF) light software was used to visualize cellular uptake of labeled micelles.

### 2.2. Preparation of hemin-loaded micelles

Hemin-loaded mPEG-*b*-p(HPMAm-$Lac_2$) micelles were prepared via the "rapid heating method" essentially as described by Neradovic et al. [32] and by Rijcken et al. [27] with some modifications. In short, the polymer was dissolved at a concentration of 2 mg/ml in 120 mM ammonium acetate pH 5 in a glass vial and stirred on ice for 1 h. 120 mM ammonium acetate pH 5 was prepared by dissolving 0.925 g of ammonium acetate in 100 ml purified water. The pH of this solution was subsequently adjusted with 0.1 N HCl to pH 5. This solvent was used as at this pH the hydrolysis of the lactate groups is limited, resulting in a high stability of the micelles [36]. Next the mixture was stored overnight at 4 °C and subsequently stirred for 15 min on ice and kept on ice until the micelles were made. This procedure was followed to ensure that the polymer solution remained below the critical micelle temperature (CMT) of 4 °C. Solutions of 0.4–2 mg/ml hemin in a mixture of DMSO:DMF (1:9 v/v) were freshly made and also kept on ice. Subsequently, 0.1 ml of hemin solution was added to 0.9 ml of polymer solution, and vortexed for 4 s and the hemin/polymer mixture was then transferred into a water bath of 50 °C and hemin loaded micelles were formed under vigorous

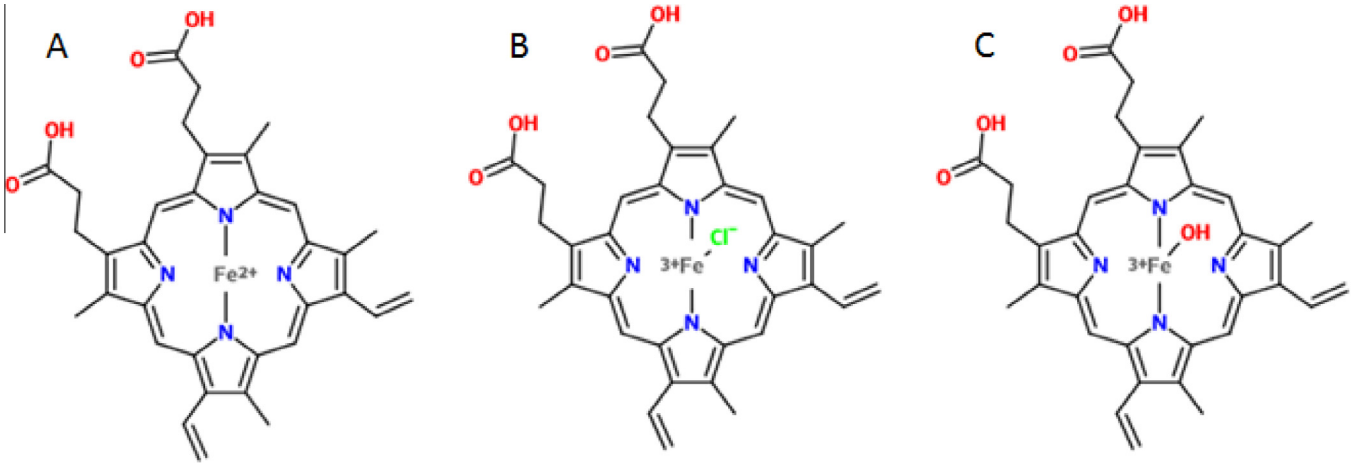


**Fig. 1.** Molecular structure of (A) heme; (B) hemin and (C) hematin.

shaking for 1 min. Finally, after cooling to room temperature, the hemin-loaded micelles were filtered through a 0.45 μm filter to remove precipitated, non-encapsulated, hemin.

### 2.3. Determination of hemin loading capacity and encapsulation efficiency of the micelles

The concentration of hemin encapsulated in the micelles was measured via UV-spectrophotometric analysis (Spectrostar BMG Labtech). A sample of the micellar dispersion was diluted 10× in DMSO to disintegrate the micelles and solubilize the encapsulated hemin. A calibration curve of hemin standards was made in a concentration range of 0–50 μg/ml in DMSO. The samples and the standards were measured at a wavelength of 388 nm and the concentration of encapsulated hemin was determined using the calibration curve. The encapsulation efficiency (EE%) and the loading capacity (LC%) were calculated as follows:

$$EE = \frac{\text{concentration hemin measured}}{\text{concentration of the hemin added}} \times 100\%$$

$$LC = \frac{\text{concentration hemin measured}}{\text{concentration (hemin measured + polymer added)}} \times 100\%$$

### 2.4. Dynamic light scattering

The size and polydispersity index of the micelles were measured using dynamic light scattering (DLS) using a ALV/CGS-3 (ALV gmbh, Langen Germany) with a JDS Uniphase laser functioning at a wavelength of 632.8 nm, an optical fiber-based detector, a digital ALV/LSE 5003 correlator and a temperature controller set at 25 °C. The refractive index and viscosity used for the data treatment were respectively 1.333 and 0.89 cp. All measurements were performed at a 90° angle. The Z-average mean particle size ($Z_{ave}$) and the polydispersity were calculated using the ALV-60 0 V.3.X software. The samples were made by diluting 10–20 μl micelle dispersion in 1 ml of 120 mM ammonium acetate pH 5.

### 2.5. Physical state of hemin in the micelles

Hemin-loaded micelles with the highest loading capacity and encapsulation efficiency were made as described in Section 2.2. In detail, 0.1 ml of 120 μg/ml hemin in DMSO:DMF (1:9) was added to 0.9 ml of 1.8 mg/ml mPEG-*b*-p(HPMAm-$Lac_2$) in 120 mM ammonium acetate pH 5. Hemin was also dissolved in DMSO to obtain the same hemin concentration as the diluted micelle sample. UV–vis spectra (λ 200–700 nm) of the solutions were recorded.

### 2.6. Stability of hemin-loaded micelles

The stability of hemin-loaded micelles at pH 2 and pH 7.4 at 37 °C was determined by measuring the particle size ($Z_{ave}$) and polydispersity for 17 h. For the stability at pH 2, the hemin-loaded micelles were formed in 120 mM ammonium acetate pH 5 as described in Section 2.2 followed by lowering to pH 2 by addition of 4 M HCl. To determine the stability of the hemin-loaded micelles at pH 7.4, the polymer was dissolved in PBS pH 7.4 containing 8.2 g NaCl, 3.1 g $Na_2HPO_4{\cdot}12H_2O$ and 0.3 g $NaH_2PO_4$ $2H_2O$ per liter.

### 2.7. Synthesis of mPEG-b-p((HPMAm-$Lac_2$)-co-RhodMA)

Rhodamine labeled mPEG-*b*-p(HPMAm-$Lac_2$) was synthesized according to a previously reported polymerization procedure [33,34]. In short, methacryloxyethyl thiocarbamoyl rhodamine B and HMPA-$Lac_2$ (molar ratio 1:99) together with $(mPEG)_2$ –ABCPA macroinitiator in a molar ratio of initiator to monomer of 1:150 were dissolved in 3 ml acetonitrile (ACN) at a scale of 700 mg monomer. The mixture was flushed for 15 min with nitrogen at room temperature and subsequently stirred overnight at 70 °C. Next, the formed polymer was precipitated in diethyl ether and then dissolved in water. Dialysis was done for two days against ACN:$H_2O$ (1:1), three days against THF:$H_2O$ (1:1) and 4 days against $H_2O$ in order to purify the polymer and remove low molecular weight impurities. The dialysis medium was refreshed 3 times a day. After dialysis, the rhodamine labeled polymer was recovered by lyophilization and characterized via $^1H$ NMR and GPC as described by Soga et al. [26] and Rijcken et al. [27].

### 2.8. In vitro cell studies

#### 2.8.1. Caco-2 cell culture

The Caco-2 cells were cultured in Dulbecco's Modified Eagle's Medium (DMEM) containing 3.7 g/L sodium bicarbonate, 4.5 g/L glucose completed with 10% fetal bovine serum (FBS), 1% antibiotics/antimycotics (100 IU penicillin G sodium/ml, 100 μg/ml streptomycin sulfate and 0.25 μg/ml amphotericin B) and 1% non-essential amino acids. The cells were seeded at a density of 100,000 cells per $cm^2$ on polystyrene well plates at 37 °C in a

humidified atmosphere containing 5% $CO_2$ and were allowed to differentiate for 14 days prior to the experiments. Medium was replaced every 2–3 days.

*2.8.2. Sample preparation for cellular uptake studies*

Hemin-loaded micelles with the highest loading capacity and encapsulation efficiency were made as described in Sections 2.2 and 2.3. Multiple dispersions of 1 ml were pooled and concentrated using viva spin centrifugal concentrator tubes (cutoff 50,000 kDa, Sartorius Stedim, Germany) for 40 min at 4000g, resulting in micellar dispersions concentrated around 70 times.

The concentration of hemin in the micellar concentrate was determined by diluting the micellar dispersion 40× in PBS and then further diluting 10× in DMSO. Next, UV-spectroscopy at 388 nm was used to determine the hemin concentration. This hemin-loaded micellar dispersion was used to perform dose response and time dependent cellular uptake as well as cytotoxicity studies. The volume of the micellar dispersion needed for the dose response and time dependent uptake studies was adjusted to 150 μl with PBS and mixed with 1350 μl cell culture medium to obtain 1.5 ml sample mixtures with concentrations of 10–200 μM hemin. The hemin micellar formulations were added to the Caco-2 cells and incubated for 24 h, unless otherwise stated, at 37 °C humidified atmosphere containing 5% $CO_2$. For the iron sulfate samples or iron sulfate combined with ascorbic acid in a molar ratio of (1:5), the necessary amount was dissolved in 150 μl PBS and mixed with 1350 μl cell culture medium to obtain iron sulfate solutions with concentration ranging from 10 to 200 μM.

*2.8.3. Cellular uptake studies*

After incubation of the Caco-2 cells with hemin-loaded micelles and iron sulfate formulations for 24 h, the medium was removed and the cells were washed with PBS. The cells were then lysed with 350 μl RIPA buffer supplemented with a 1% proteinase inhibitor cocktail. The lysed cells were stored at −20 °C until analyzed. Prior to analysis, the cells were thawed and spun down at 20,000 rpm for 15 min. Next, the protein concentration of the samples was measured using a Micro BCA protein assay kit (Pierce, Rockford USA). A dilution range of 1–200 μg/ml bovine serum albumin was used for calibration. In order to assess the iron uptake, the total ferritin content of the cell lysates was measured using a double sandwiched ELISA against human ferritin kit (ab 108837 Abcam, Cambridge United Kingdom). Both the protein and ferritin assays were performed according to the manufacturer's protocol.

*2.8.4. Cell viability*

The viability of the Caco-2 cells after incubation with the different formulations was assessed using a yellow tetrazolium salt XTT colorimetric assay that measures the metabolic activity of cells as first described by Scudiero et al. [35]. In short, Caco-2 cells were seeded at a density of 20,000 cells/well in a 96 well plate and incubated at 37 °C. After 24 h, the cell culture medium was removed and replaced by an iron sample mixture of 150 μl, consisting of 100 μl medium and 50 μl made up of a volume of the different iron samples needed to obtain different concentrations adjusted with PBS. The cells were incubated for 24 h and then washed with PBS. Next, 50 μl of fresh medium and 50 μl of XTT solution were added to the cells, which were subsequently incubated for 1 h at 37 °C. Finally, the plates were measured using UV-spectroscopy at a wavelength of 490 nm and the relative cell survival after 24 h treatment was compared to non-treated Caco-2 cells.

*2.8.5. Intracellular localization of hemin-loaded micelles*

A rhodamine labeled polymer was synthesized as described in Section 2.7 and the hemin loaded mPEG-*b*-p((HPMAm-$Lac_2$)-*co*-RhodMA) micelles were prepared as described in Section 2.2 except that the rhodamine labeled polymer was dissolved in PBS pH 7.4 instead of 120 mM ammonium acetate. The Caco-2 cells were seeded at a density of 50,000 cells/well in a 16-well glass chamber slide system (Lab-Tek; chamber slide™ system 178599) and grown for 5 days in an incubator at 37 °C to reach 80% confluency. The rhodamine micelles dispersion was then diluted 4× with phenol red free DMEM culture medium. Next, the cells were incubated with the diluted dispersion for 3 h and subsequently the medium was replaced and the cells were washed twice with PBS. The Caco-2 cells were subsequently fixed with 4% paraformaldehyde for 30 min, the fixative was then discarded and the cells were washed again twice with PBS. Binding buffer was made by preparing a stock solution of 50 mg Saponin from Sigma Aldrich and 100 mg BSA in 50 ml PBS. After the Caco-2 cells were fixed they were quenched for 10 min with 50 nM $NH_4Cl$ dissolved in water and washed twice with PBS. The binding buffer was then added to the cells and incubated for 30 min at room temperature. Next the primary antibody LAMP-1 to stain lysosomes, was dissolved in binding buffer (1 μg/ml). This antibody solution was then pipetted onto the cells and incubated for 60 min at room temperature. Subsequently, the secondary antibody Alexa-488 was used to detect the binding of the primary antibody and was dissolved in binding buffer (10 μg/ml). After 60 min of incubation with the primary antibody at room temperature, the Caco-2 cells were washed 4× with PBS and the secondary antibody conjugated to Alexa-488 was added and incubated for 60 min. Finally, the cells were washed 3 times with PBS and once with Milli-Q ultrapure water and then mounted on the glass chamber slide system using FluorSave from Calbiochem, San Diego. Confocal microscopy was used to visualize the uptake of the rhodamine labeled micelles by measuring the red color within the cells and also to visualize lysosomes as the LAMP-1 antibody staining produced a green color.

## 3. Results and discussion

*3.1. Characterization of mPEG-b-p(HPMAm-$Lac_2$) block copolymer*

Synthesis and characterization of mPEG(5000)-*b*-p(HPMAm-Lac2) block copolymer were performed and characterized as described by Soga et al. [26,36]. The polymer was obtained in a yield of 73% and the number average molecular weight as determined by NMR analysis was 17,400 g/mol. GPC analysis of the polymer (using PEG calibration) gave a number average molecular weight of 18,500 g/mol, the weight average molecular weight was 37,200 g/mol and the dispersity (*Đ*) was 2.0 which is close to earlier reported data [36].

*3.2. Preparation and characterization of hemin loaded micelles*

Hemin-loaded micelles with different loadings of hemin were prepared as described in Section 2.2 by addition of a small volume of hemin in DMSO to a cold aqueous polymer solution (1.8 mg/ml, which is far above the critical micelle concentration (CMC) of 0.015 mg/ml as reported for this polymer [36]), followed by rapidly heating the solution to 50 °C. After filtration to remove non-encapsulated hemin, the obtained particles were characterized for hemin loading, size and size distribution. When no polymer was present, the addition of the DMSO/hemin solution to water resulted in the formation of large aggregates as shown in Fig. 2C. In contrast, when adding the hemin solution to the polymer solution the encapsulation capacity of the micelles was obvious since a brownish[2] micellar dispersion free of aggregates was obtained (Fig. 2D).

[2] For interpretation of color in Fig. 2, the reader is referred to the web version of this article.

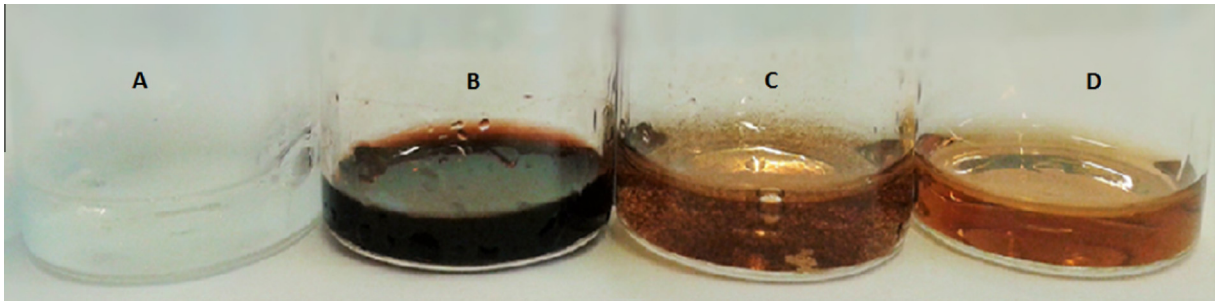


**Fig. 2.** (A) mPEG-p(HPMAm-Lac$_2$) dissolved in 120 mM ammonium acetate (2 mg/ml); (B) hemin dissolved in DMSO:DMF 1:9 (1.2 mg/ml); (C) hemin in DMSO:DMF 1:9 (1.2 mg/ml) of which 0.1 ml was added to 0.9 ml of 120 mM ammonium acetate buffer; (D) hemin-loaded micelles prepared by addition of 0.1 ml of 120 μg/ml of hemin in DMSO:DMF 1:9–0.9 ml of 1.8 mg/ml mPEG-b-p(HPMAm-Lac$_2$).

Fig. 3 shows the loading of hemin in mPEG-*b*-p(HPMAm-Lac$_2$) micelles for three independently prepared micellar dispersions per hemin concentration with corresponding standard deviations in order to obtain insight into the batch-to-batch variability. Fig. 3A demonstrates that the highest encapsulation was achieved by adding 120 μg/ml of hemin in DMSO to 1.8 mg/ml polymer solution in water. The loading capacity (LC) and encapsulation efficiency (EE) for this formulation were 3.9% and 61.4%, respectively. Fig. 3A also shows that a higher concentration of hemin resulted in a decreasing EE. This is probably due to the fact that there is not enough polymer present to encapsulate the hemin, therefore resulting in saturation of the micelles with hemin and the formation of hemin aggregates with the excess hemin subsequently being filtered away [37,38].

Fig. 3A further shows that the loading capacity increased from 2.5% at a hemin concentration of 40 μg/ml to 3.9% at a hemin concentration of 120 μg/ml and then leveled off, which is probably due to saturation of the micelles with hemin. Fig. 3B demonstrates that when increasing the hemin concentration, the average size of the micelles also increased from 75 nm to 140 nm. The particle size at the highest hemin encapsulation was 116 nm and the polydispersity index was 0.19.

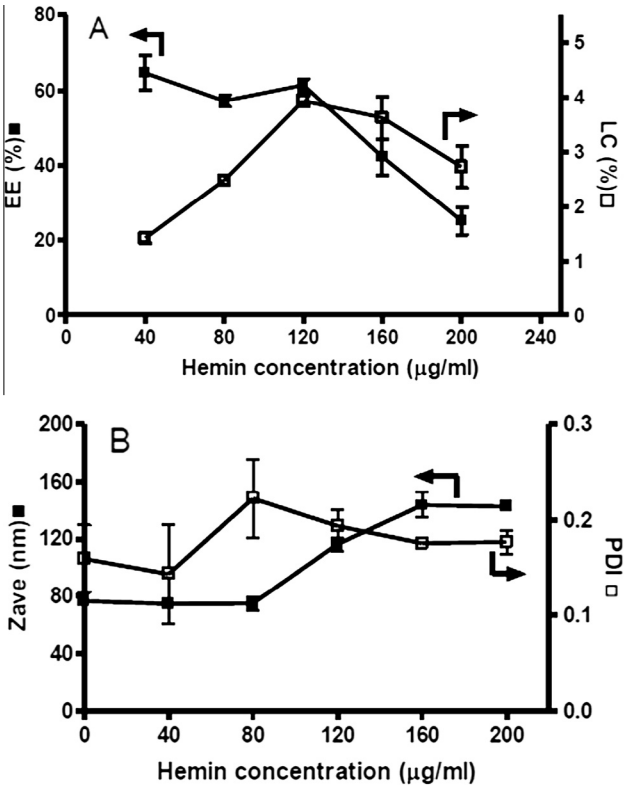


**Fig. 3.** Loading of hemin in mPEG-p(HPMAm-Lac$_2$) micelles; (A) encapsulation efficiency on the left axis and loading capacity on the right axis and (B) Z-average diameter and polydispersity of hemin loaded micelles. Results represent mean ± standard deviation of three independently prepared samples.

### 3.3. Physical state of hemin in micelles

Hemin loaded-micelles were prepared as described in Section 2.2 and subsequently diluted ten times with ammonium acetate pH 5 to obtain a dispersion with a hemin concentration of 11.4 μM and a polymer concentration of 0.18 mg/ml. The polymer concentration was above the CMC of 0.015 mg/ml [36], in order to ensure that the micelles remain intact during measurement. As control, hemin was dissolved in DMSO to obtain molecularly dissolved hemin at the same concentration as the diluted micelle sample.

Fig. 4 shows for hemin dissolved in DMSO the so-called Soret- or B band at a maximum of 404 nm, which is common for metalloporphyrins [39,40]. Fig. 4 further shows that the absorption for hemin loaded micelles is significantly broadened as compared to the absorption of hemin solubilized in DMSO. This can be ascribed to the aggregation of hemin in the micelles as previously reported for a silicon phthalocyanine photosensitizer loaded in mPEG-*b*-p(HPMAm-Lac$_2$) micelles [34]. Furthermore, the soret band for the hemin loaded-micelles shifted to lower wavelengths of respectively 385 nm compared to hemin dissolved in DMSO (404 nm). This shift is also known as a hypsochromic shift and is indicative for H-aggregation. Metalloporphyrins that form H-aggregates which are caused by strong metal to porphyrin orbital interaction are also called hypsoporphyrins. This interaction results in an enhanced porphyrin $\pi$-$\pi^*$ energy separation which subsequently leads to the hypsochromic shift as observed in Fig. 4 [41,42]. The results presented in Fig. 4 imply that hemin is most likely present in an aggregate state within the micelles which can be beneficial as premature release of hemin when transiting through the digestive system is retarded.

### 3.4. Stability of hemin-loaded mPEG-b-p(HPMAm-Lac$_2$) micelles

In order for the hemin micelles to be effective for therapy, they should not disintegrate in the upper part of the digestive system and therefore the stability of the particles was examined at both pH 2 (stomach) and pH 7.4 (duodenum). Hemin loaded mPEG-*b*-p(HPMAm-Lac$_2$) micelles with the highest encapsulation and loading capacity (Fig. 3A) were used for these studies.

Fig. 5A illustrates that at pH 2 the size of the micelles slightly increases from 143 to 199 nm upon incubation for 17 h at 37 °C, whereas at pH 7.4 (Fig. 5B) the size remained constant in time.

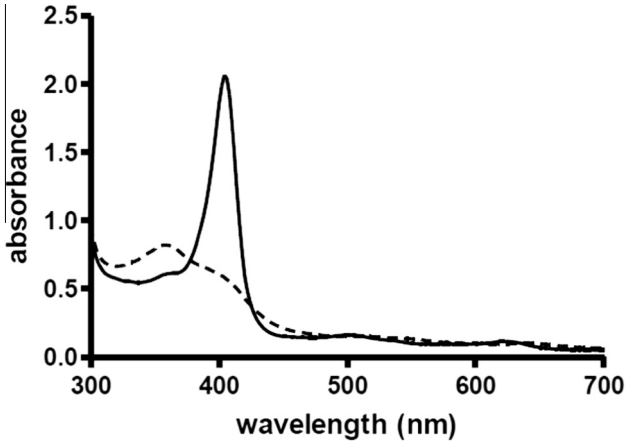


**Fig. 4.** UV–vis spectra of hemin; (—) hemin (11.4 μM) in DMSO, (--) hemin loaded micelles (11.4 μM of hemin) in 120 mM ammonium acetate pH 5.

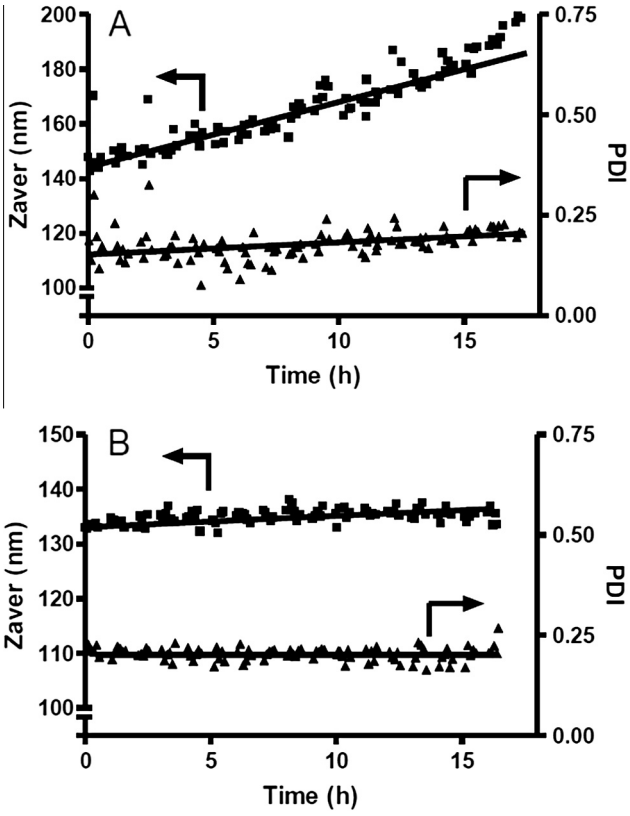


**Fig. 5.** Z-average size ($Z_{ave}$) and polydispersity (PDI) of hemin micelles at 37 °C as a function of time at pH 2 (figure A) and at pH 7.4 (figure B); A: micelles were prepared at pH 5 as described in Section 2.2 and then adjusted to pH 2 with 4 M HCl; B: micelles were prepared using a polymer solution in PBS pH 7.4 as described in Section 2.6.

The polydispersity remained constant in time at both pH's, at an average of 0.18 at pH 2 and 0.21 at pH 7.4. The scattered intensity data provided as supporting information (Fig. S2) demonstrate that at pH 2 the scattered intensity slowly decreases in time indicating slow degradation of the micelles, while at pH 7.4 the scattered intensity of the micelles remains constant throughout the measurement. However, during the first three hours that cover the common transit time in the stomach [43,44], the average size and scattered intensity remained almost constant at pH 2. At pH 7.4 the micelles were stable up to 17 h which could be beneficial for the uptake by the enterocytes after their oral administration.

### *3.5. Cellular in vitro uptake of hemin-loaded mPEG-b-p(HPMAm-Lac$_2$) micelles*

To study the feasibility of hemin-loaded micelles as formulation for oral iron delivery, several experiments were performed on Caco-2 cell cultures. The Caco-2 cell line has been extensively used to study nutrient and drug transport, as these cells upon differentiation express a comparable microvilli brush border with functionality similar to the enterocytes present in the small intestines [45,46]. Ferritin is also a well-known marker for cellular iron uptake as it is the protein that stores iron when not needed elsewhere in the organism [47]. Once the Hemin loaded micelles are internalized by cells and the hemin is released, it is degraded by the enzyme heme oxygenase which is present on the endoplasmic reticulum resulting in the formation of $Fe^{2+}$, biliverdin and carbon monoxide [48]. Subsequently the iron in the cytoplasm enters the common iron pool and is then transported to the bloodstream via the protein ferroportin. The excess iron that is not required to enter in the circulatory system is stored in the cytosolic protein ferritin [8,49]. The regulation of ferritin synthesis occurs via the translation of ferritin H and L mRNA's in the presence of accessible iron in the labile iron pool which can be defined as a cell chelatable pool consisting of mainly $Fe^{2+}$ associated with various ligands with an affinity for iron [50–52]. This results in an increase or decrease in ferritin synthesis and thus ferritin expression when iron levels are high or down regulated when iron levels are low [8,53]. In the present study, Caco-2 cells were incubated with dispersions of hemin-loaded micelles with different concentrations, as well as with iron sulfate or iron sulfate in combination with ascorbic acid. Also, a cytotoxicity assay was done to assess the cytocompatibility of the formulations.

#### *3.5.1. Uptake of hemin-loaded mPEG-b-p(HPMAm-Lac$_2$) micelles by Caco-2 cells*

In order to study uptake of hemin-loaded micelles, mPEG-*b*-p((HPMAm-Lac$_2$)-*co*-RhodMA) was synthesized as described in Section 2.7. GPC analysis (Fig. 6) equipped with both RI- and UV-detectors was performed to determine the number average molecular weight and the amount of free rhodamine in the sample. The number average molecular weight ($M_n$) using PEG standards for calibration was 23,500 g/mol; $M_w/M_n = 2.0$. Furthermore GPC analysis showed that the amount of free label was less than 3%.

Rhodamine labeled mPEG-*b*-p(HPMAm-Lac$_2$) micelles were prepared as described in Section 2.8.5 to perform cellular uptake studies.

In order to observe whether hemin-loaded micelles were taken up by the Caco-2 cells, confocal microscopy was performed using rhodamine labeled hemin-micelles and the commonly used lysosome marker LAMP-1 [54]. Fig. 7B depicts that after an incubation time of 3 h, the cells take up the labeled micelles, but Fig. 7C shows that most of the green fluorescence of the lysosomes does not overlap with the red rhodamine fluorescence. This indicates that the rhodamine micelles were not present in lysosomal vesicles as would be expected if the uptake mechanism was via endocytosis [55]. Similar results were also obtained by Rijcken et al. [34] who incubated murine melanoma B16F10 cells with mPEG-*b*-p((HPMAm-Lac$_2$)-*co*-RhodMA) micelles to investigate the cellular uptake of these particles. Furthermore, the particles studied in this paper had an average size of 116 nm as shown in Fig. 3B, which is well above the optimal particle size of 25–30 nm for endocytosis according to a study performed by Zhang et al. [56]. Nevertheless uptake of hemin into the cells in its free form is not expected because of its low aqueous solubility and therefore the high levels of ferritin that are formed after incubation of the hemin-micelles with the cells, as shown in Section 3.5.2, are probably due to the internalized micelles. Talelli et al. [57], also demonstrated that

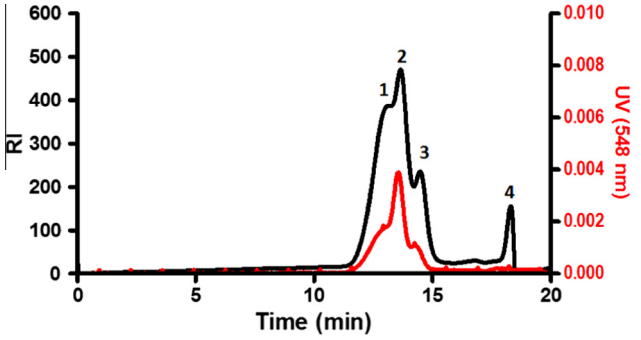


**Fig. 6.** GPC profile (1) mPEG-*b*-p((HPMAm-Lac$_2$)-*co*-RhodMA); (2) traces of the PEG-macroinitiator; (3) free PEG; (4) injection peak. The red line is the UV signal at 548 nm and black line is RI signal. (For interpretation of the references to color in this figure legend, the reader is referred to the web version of this article.)

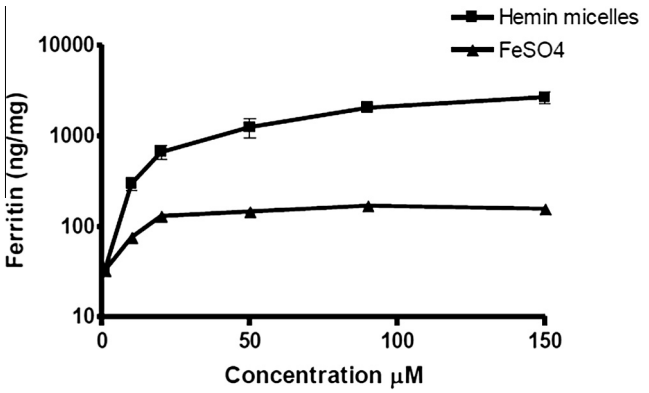


**Fig. 8.** Formation of ferritin (in ng/mg cellular protein) by caco-2 cells upon incubation with hemin loaded mPEG-b-p(HPMAm-Lac$_2$) micelles or iron sulfate for 24 h at 37 °C. Results represent mean ± standard deviation of three experiments.

similar rhodamine labeled micelles, both non-targeted and EGa1 nanobody targeted were indeed taken up by 14C cells. Sahay et al. [58] discussed the various pathways that nanoparticles composed of different materials use to enter cells, including nanomaterials that are able to bypass early endosomes and lysosomes. However some of these mechanisms are not fully understood, but up to date any of the endocytic pathways are considered the main cellular uptake mechanism for micelles [59].

### 3.5.2. Ferritin expression after in vitro uptake of iron complex

Fig. 8 presents the ferritin expression after incubating the Caco-2 cells for 24 h with dispersions of hemin-loaded micelles or iron sulfate. After incubating the cells with medium containing iron sulfate in various concentrations, ferritin values reached a maximum of 250 ng/mg protein at a concentration of 150 μM. It can also be observed that at this iron sulfate concentration the expression of intracellular ferritin reached a plateau.

Importantly, when the cells were incubated with medium containing hemin-loaded micelles, ferritin values of 2500 ng/mg protein were observed, which are more than 10-fold higher than those obtained when incubating the cells with iron sulfate. This observation is in accordance with a previous study in which it has been reported that heme iron is probably being taken up more efficiently by Caco-2 cells than non-heme iron such as iron salts [11].

Additional experiments were performed to study the effect of combining ascorbic acid (vitamin C), a vitamin that beneficially enhances iron uptake [60].

Fig. 9 shows that when ascorbic acid was added to the medium, a substantial higher ferritin formation was observed, confirming literature claims [60]. Furthermore, it can be observed that there were no significant differences between ferritin expressed by cells incubated with iron sulfate supplemented with ascorbic acid or hemin loaded micelles. However, ascorbic acid is a strong reductant which in excess could lead to the formation of undesired high $Fe^{2+}$ amounts and result in possible pro-oxidative activity [61,62]. In addition, we investigated possible cytotoxic effects of the different iron formulations using the XTT assay. The results shown in Fig. 10 demonstrate that incubating Caco-2 cells with hemin-loaded micelles with a concentration up to 150 μM, has no effect on the cell viability whereas iron sulfate combined with ascorbic acid was clearly cytotoxic, with an $IC_{50}$ value of 50 μM.

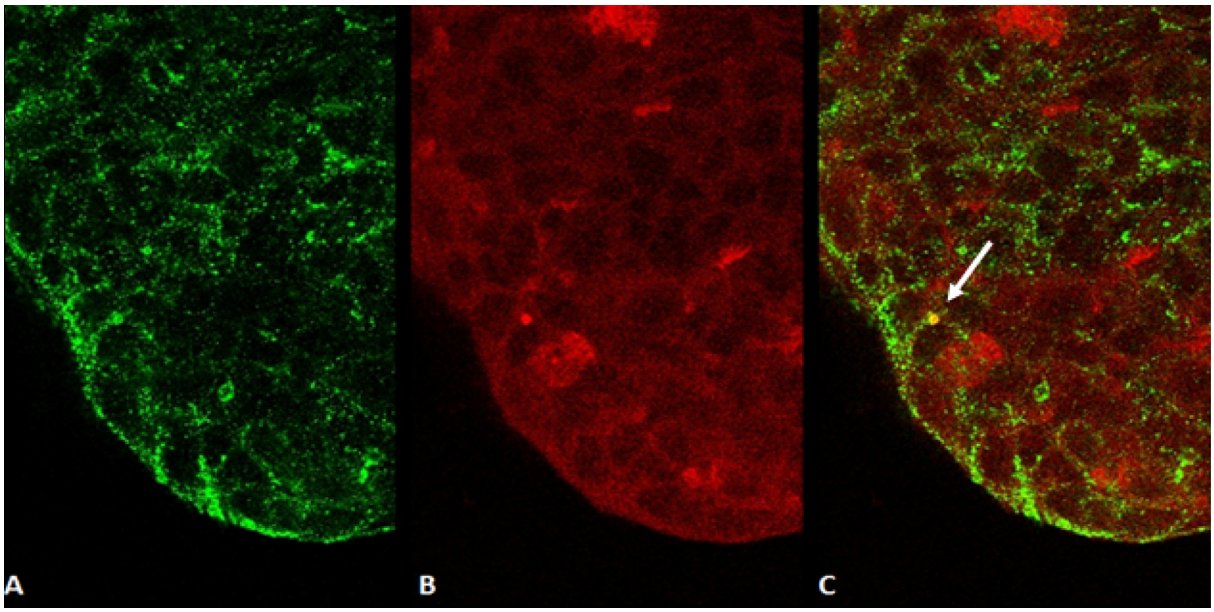


**Fig. 7.** Confocal microscopy of caco-2 cells incubated for 3 h at 37 °C with rhodamine labeled hemin-micelles. A: lysosome staining in green; B: rhodamine labeled micelles in red; C: overlap of lysosome staining and rhodamine. (For interpretation of the references to color in this figure legend, the reader is referred to the web version of this article.)

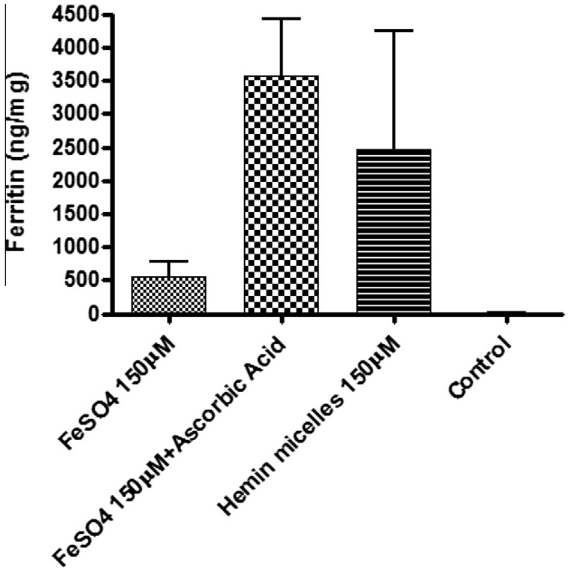


**Fig. 9.** Formation of ferritin (in ng/mg cellular protein) by caco-2 cells after 24 h of incubation with 150 µM of hemin loaded mPEG-b-p(HPMAm-$Lac_2$) micelles, iron sulfate, iron sulfate plus ascorbic acid in a molar ratio of 1:5, and DMEM medium only. Results represent mean ± standard deviation of three experiments.

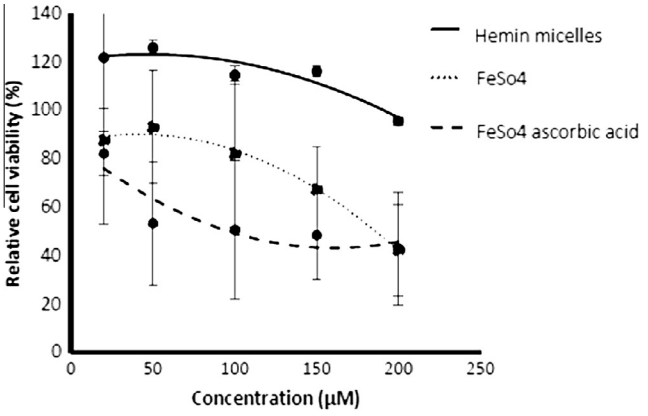


**Fig. 10.** Viability of caco-2 cells upon incubation of different concentrations of Hemin-loaded micelles; Iron sulfate; Iron sulfate:Ascorbic acid (1:5) and empty micelles. Results represent mean ± standard deviation of three experiments.

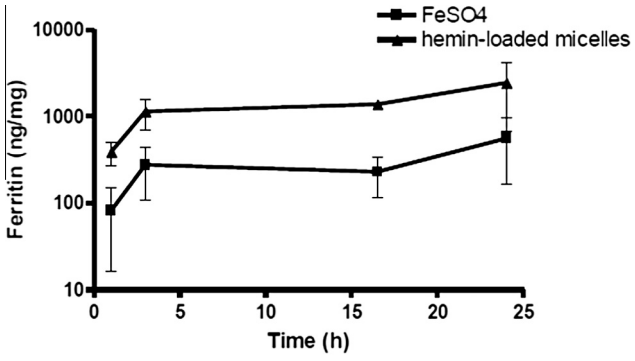


**Fig. 11.** Formation of ferritin in ng/mg cellular protein as function of incubation time of caco-2 cells with hemin-loaded micelles (150 µM) and iron sulfate (150 µM). Results represent mean ± standard deviation of three experiments.

### *3.5.3. Kinetics of ferritin formation in Caco-2 cells after incubation of iron samples*

The kinetics of ferritin formation was investigated by incubating the Caco-2 cells with iron sulfate and hemin-loaded micelles with a concentration of 150 µM. The hemin-loaded micellar dispersion was made from 120 µg hemin/ml in 1.8 mg/ml polymer as described in Section 2.8.2. Fig. 11 illustrates that the amount of ferritin reached a maximum already after 3 h upon incubation with both formulations at 37 °C. After this incubation time there is no significant difference in formation of ferritin.

In many previous studies using Caco-2 cells as a model cell line to investigate iron uptake, the cells were harvested after 24 h upon incubation with iron supplements in order to allow ferritin formation [47,63]. However, here we demonstrate that 3 h is sufficient to reach a maximum of ferritin formation upon incubation with both hemin-loaded micelles and iron sulfate.

## 4. Conclusions

The present study shows that hemin can successfully be loaded in mPEG-*b*-p(HPMAm-$Lac_2$) micelles forming water dispersible particles with an average size of around 100 nm. The hemin-loaded micelles demonstrated to remain stable up to 3 h at pH 2 and 17 h at pH 7.4. Importantly, upon incubation in Caco-2 cells the hemin-loaded micelles gave superior ferritin formation up to 10× times higher than when compared to the commonly used iron supplement iron sulfate. The new hemin formulation presented in this paper is therefore a promising formulation for iron oral delivery.

## Acknowledgements

This research was financially supported by Vifor (international) Ltd., St. Gallen, Switzerland.

## Appendix A. Supplementary material

Supplementary data associated with this article can be found, in the online version, at http://dx.doi.org/10.1016/j.ejpb.2016.09.002.

## References

[1] Bruno de Benoist, Erin McLean, Ines Egli, Cogswell, Worldwide Prevalence of Anaemia 1993–2005: WHO Global Database on Anaemia, 2008, ISBN 978 92 4 159665 7.
[2] S. Yun, J.P. Habicht, D.D. Miller, R.P. Glahn, An in vitro digestion/Caco-2 cell culture system accurately predicts the effects of ascorbic acid and polyphenolic compounds on iron bioavailability in humans, J. Nutr. 134 (2004) 2717–2721.
[3] E.C. Theil, Iron homeostasis and nutritional iron deficiency, J. Nutr. 141 (2011) 724S–728S.
[4] R.P. Glahn, M. Rassier, M.I. Goldman, O.A. Lee, J. Cha, A comparison of iron availability from commercial iron preparations using an in vitro digestion/Caco-2 cell culture model, J. Nutr. Biochem. 11 (2000) 62–68.
[5] G.J. Anderson, D.M. Frazer, G.D. McLaren, Iron absorption and metabolism, Curr. Opin. Gastroenterol. 25 (2009) 129–135.
[6] P. Santiago, Ferrous versus ferric oral iron formulations for the treatment of iron Deficiency: a clinical overview, Sci. World J. 2012 (2012) 5.
[7] B.K. Fuqua, C.D. Vulpe, G.J. Anderson, Intestinal iron absorption, J. Trace Elem. Med. Biol. 26 (2012) 115–119.
[8] R. Evstatiev, C. Gasche, Iron sensing and signalling, Gut 61 (2012) 933–952.
[9] J. Wang, K. Pantopoulos, Regulation of cellular iron metabolism, Biochem. J. 434 (2011) 365–381.
[10] A.A. Khan, J.G. Quigley, Control of intracellular heme levels: heme transporters and heme oxygenases, Biochim. Biophys. Acta - Mol. Cell Res. 2011 (1813) 668–682.
[11] S. Miret, S. Tascioglu, M. van der Burg, L. Frenken, W. Klaffke, In vitro bioavailability of iron from the heme analogue sodium iron chlorophyllin, J. Agric. Food Chem. 58 (2010) 1327–1332.
[12] P. Villarroel, S. Flores, F. Pizarro, D. de Romaña, M. Arredondo, Effect of dietary protein on heme iron uptake by Caco-2 cells, Eur. J. Nutr. 50 (2011) 637–643.

[13] D.S. Kalinowski, D.R. Richardson, The evolution of iron chelators for the treatment of iron overload disease and cancer, Pharmacol. Rev. 57 (2005) 547–583.
[14] Comparison of oral iron supplements, Pharmacist's Lett/Prescriber's Lett 24 (8) (2008) 240811.
[15] M. Shayeghi, G.O. Latunde-Dada, J.S. Oakhill, A.H. Laftah, K. Takeuchi, N. Halliday, et al., Identification of an intestinal heme transporter, Cell 122 (n.d.) 789–801.
[16] C. Cao, C. Thomas, K. Insogna, K. O'Brien, Duodenal expression of heme and non-heme iron transporters and tissue partitioning of dietary heme and non-heme iron in a rat mode of iron overload, FASEB J. 28 (2014), meeting abstract 246.8.
[17] T. Korolnek, I. Hamza, Like iron in the blood of the people: the requirement for heme trafficking in iron metabolism, Front. Pharmacol. 5 (2014) 126.
[18] T.J. Egan, E. Hempelmann, W.W. Mavuso, Characterisation of synthetic β-haematin and effects of the antimalarial drugs quinidine, halofantrine, desbutylhalofantrine and mefloquine on its formation, J. Inorg. Biochem. 73 (1999) 101–107.
[19] A.C. Hunter, J. Elsom, P.P. Wibroe, S.M. Moghimi, Polymeric particulate technologies for oral drug delivery and targeting: a pathophysiological perspective, Nanomedicine 8 (2012) S5–S20.
[20] S. Mazzaferro, K. Bouchemal, G. Ponchel, Oral delivery of anticancer drugs III: formulation using drug delivery systems, Drug Discov. Today 18 (2013) 99–104.
[21] G. Gaucher, P. Satturwar, M.-C. Jones, A. Furtos, J.-C. Leroux, Polymeric micelles for oral drug delivery, Eur. J. Pharm. Biopharm. 76 (2010) 147–158.
[22] K. Thanki, R.P. Gangwal, A.T. Sangamwar, S. Jain, Oral delivery of anticancer drugs: challenges and opportunities, J. Control. Release 170 (2013) 15–40.
[23] L. Zhang, S. Wang, M. Zhang, J. Sun, Nanocarriers for oral drug delivery, J. Drug Target. 21 (2013) 515–527.
[24] L. Mei, Z. Zhang, L. Zhao, L. Huang, X.-L. Yang, J. Tang, et al., Pharmaceutical nanotechnology for oral delivery of anticancer drugs, Adv. Drug Deliv. Rev. 65 (2013) 880–890.
[25] C. Deng, Y. Jiang, R. Cheng, F. Meng, Z. Zhong, Biodegradable polymeric micelles for targeted and controlled anticancer drug delivery: promises, progress and prospects, Nano Today 7 (2012) 467–480.
[26] O. Soga, C.F. van Nostrum, W.E. Hennink, Poly(N-(2-hydroxypropyl) methacrylamide mono/di Lactate): a new class of biodegradable polymers with tuneable thermosensitivity, Biomacromolecules 5 (2004) 818–821.
[27] C.J.F. Rijcken, T.F.J. Veldhuis, A. Ramzi, J.D. Meeldijk, C.F. van Nostrum, W.E. Hennink, Novel fast degradable thermosensitive polymeric micelles based on PEG-block-poly(N-(2-hydroxyethyl)methacrylamide-oligolactates), Biomacromolecules 6 (2005) 2343–2351.
[28] D. Schmaljohann, Thermo- and pH-responsive polymers in drug delivery, Adv. Drug Deliv. Rev. 58 (2006) 1655–1670.
[29] S.R. MacEwanand, A. Chilkoti, Applications of elastin-like polypeptides in drug delivery, J. Control. Release 190 (2014) 314–330.
[30] M. Talelli, C.J.F. Rijcken, T. Lammers, P.R. Seevinck, G. Storm, C.F. van Nostrum, et al., Superparamagnetic iron oxide nanoparticles encapsulated in biodegradable thermosensitive polymeric micelles: toward a targeted nanomedicine suitable for image-guided drug delivery, Langmuir 25 (2009) 2060–2067.
[31] O. Naksuriya, Y. Shi, C.F. van Nostrum, S. Anuchapreeda, W.E. Hennink, S. Okonogi, HPMA-based polymeric micelles for curcumin solubilization and inhibition of cancer cell growth, Eur. J. Pharm. Biopharm. 94 (2015) 501–512.
[32] D. Neradovic, O. Soga, C.F. Van Nostrum, W.E. Hennink, The effect of the processing and formulation parameters on the size of nanoparticles based on block copolymers of poly(ethylene glycol) and poly(N-isopropylacrylamide) with and without hydrolytically sensitive groups, Biomaterials 25 (2004) 2409–2418.
[33] O. Soga, C.F. van Nostrum, M. Fens, C.J.F. Rijcken, R.M. Schiffelers, G. Storm, et al., Thermosensitive and biodegradable polymeric micelles for paclitaxel delivery, J. Control. Release 103 (2005) 341–353.
[34] C.J.F. Rijcken, J.-W. Hofman, F. van Zeeland, W.E. Hennink, C.F. van Nostrum, Photosensitiser-loaded biodegradable polymeric micelles: preparation, characterisation and in vitro PDT efficacy, J. Control. Release 124 (2007) 144–153.
[35] D.A. Scudiero, R.H. Shoemaker, K.D. Paull, A. Monks, S. Tierney, T.H. Nofziger, et al., Evaluation of a soluble tetrazolium/formazan assay for cell growth and drug sensitivity in culture using human and other tumor cell lines, Cancer Res. 48 (1988) 4827–4833.
[36] O. Soga, C.F. van Nostrum, A. Ramzi, T. Visser, F. Soulimani, P.M. Frederik, et al., Physicochemical characterization of degradable thermosensitive polymeric micelles, Langmuir 20 (2004) 9388–9395.
[37] M.C. Jones, J.C. Leroux, Polymeric micelles – a new generation of colloidal drug carriers, Eur. J. Pharm. Biopharm. 48 (1999) 101–111.
[38] M. Yokoyama, A. Satoh, Y. Sakurai, T. Okano, Y. Matsumura, T. Kakizoe, et al., Incorporation of water-insoluble anticancer drug into polymeric micelles and control of their particle size, J. Control. Release 55 (1998) 219–229.
[39] V. Srinivas, Ch. Mohan Rao, Time profile of hemin aggregation: an analysis, Biochem. Int. 21 (1990) 849–855.
[40] M.E. Lombardo, L.S. Araujo, A.B. Ciccarelli, A. Batlle, A spectrophotometric method for estimating hemin in biological systems, Anal. Biochem. 341 (2005) 199–203.
[41] S. Hirohara, M. Obata, S. Ogata, K. Kajiwara, C. Ohtsuki, M. Tanihara, et al., Sugar-dependent aggregation of glycoconjugated chlorins and its effect on photocytotoxicity in HeLa cells, J. Photochem. Photobiol. B Biol. 84 (2006) 56–63.
[42] M. Prushan, Absorption and Fluorescence Spectroscopy of Tetraphenyl Porphyrin and Metallo-tertraphenylporphyrin, 2005, pp. 1–9. <http://www.lasalle.edu/>.
[43] M. Camilleri, L.J. Colemont, S.F. Phillips, M.L. Brown, G.M. Thomforde, N. Chapman, A.R. Zinsmeister, Human gastric emptying and colonic filling of solids characterized by a new method, Am. J. Physiol. – Gastr. Liver Physiol. 257 (1989) G284–G290.
[44] L.P. Degen, S.F. Phillips, Variability of gastrointestinal transit in healthy women and men, Gut 39 (1996) 299–305.
[45] M. Pinto, S. Robine-Leon, M. Appay, M. Kedinger, N. Triadou, E. Dussaulx, B. Lacroix, P. Simon-Assmann, K. Haffen, J. Fogh, A. Zweibaum, Biol. Cell 47 (1983) 323–330.
[46] B. Press, D. Di Grandi, Permeability for intestinal absorption: Caco-2 assay and related issues, Curr. Drug Metab. 9 (2008) 893–900.
[47] R.P. Glahn, O.A. Lee, A. Yeung, M.I. Goldman, D.D. Miller, Caco-2 cell ferritin formation predicts nonradiolabeled food iron availability in an in vitro digestion/Caco-2 cell culture model, J. Nutr. 128 (1998) 1555–1561.
[48] G. Kikuchi, T. Yoshida, M. Noguchi, Heme oxygenase and heme degradation, Biochem. Biophys. Res. Commun. 338 (2005) 558–567.
[49] J. Hooda, A. Shah, L. Zhang, Heme, an essential nutrient from dietary proteins, critically impacts diverse physiological and pathological processes, Nutrients 6 (2014) 1080–1102.
[50] O. Kakhlon, Z.I. Cabantchik, The labile iron pool: characterization, measurement, and participation in cellular, Free Radic. Biol. Med. 33 (2002) 1037–1046.
[51] M. Kruszewski, Labile iron pool: the main determinant of cellular response to oxidative stress, Mutat. Res. Mol. Mech. Mutagen. 531 (2003) 81–92.
[52] R.C. Hider, X. Kong, Iron speciation in the cytosol: an overview, Dalton Trans. 42 (2013) 3220–3229.
[53] F.M. Torti, S.V. Torti, Regulation of ferritin genes and protein, Blood 99 (2002) 3505–3516.
[54] T.G. Iversen, T. Skotland, K. Sandvig, Endocytosis and intracellular transport of nanoparticles: present knowledge and need for future studies, Nano Today 6 (2011) 176–185.
[55] I. Mellman, Endocytosis and molecular, Annu. Rev. Cell Dev. Biol. 12 (1996) 575–625.
[56] S. Zhang, J. Li, G. Lykotrafitis, G. Bao, S. Suresh, Size-dependent endocytosis of nanoparticles, Adv. Mater. 21 (2009) 419–424.
[57] M. Talelli, C.J.F. Rijcken, S. Oliveira, R. van der Meel, P.M.P. van Bergen en Henegouwen, T. Lammers, et al., Nanobody — shell functionalized thermosensitive core-crosslinked polymeric micelles for active drug targeting, J. Control. Release 151 (2011) 183–192.
[58] G. Sahay, D.Y. Alakhova, A.V. Kabanov, Endocytosis of nanomedicines, J. Control. Release 145 (2010) 182–195.
[59] I. Pepić, J. Lovrić, J. Filipović-Grčić, How do polymeric micelles cross epithelial barriers?, Eur J. Pharm. Sci. 50 (2013) 42–55.
[60] J.D. Cook, M.B. Reddy, Effect of ascorbic acid intake on nonheme-iron absorption from a complete diet, Am. J. Clin. Nutr. 73 (2001) 93–98.
[61] B. Sturm, H. Laggner, N. Ternes, H. Goldenberg, B. Scheiber-Mojdehkar, Intravenous iron preparations and ascorbic acid: effects on chelatable and bioavailable iron, Kidney Int. 67 (2005) 1161–1170.
[62] I.D. Podmore, H.R. Griffiths, K.E. Herbert, N. Mistry, P. Mistry, J. Lunec, Nature 392 (1998) 559.
[63] B.I. Mergler, E. Roth, S.F.A. Bruggraber, J.J. Powell, D.I.A. Pereira, Development of the Caco-2 model for assessment of iron absorption and utilisation at supplemental levels, J. Pharm. Nutr. Sci. 2 (2012) 26–33.